

Geophysical Research Letters

RESEARCH LETTER

10.1029/2020GL091859

Key Points:

- Intense current events are distributed uniformly downstream of a quasi-parallel bow shock
- The events are associated primarily with a conversion of field energy into particle energy
- The energy processed by these events is a non-negligible fraction of the energy incident at the bow shock

Supporting Information:

- Supporting Information S1
- Data Set S1

Correspondence to:







S. Schwartz,
steven.schwartz@lasp.colorado.edu

Citation:

Schwartz, S. J., Kucharek, H., Farrugia, C. J., Trattner, K., Gingell, I., Ergun, R. E., et al. (2021). Energy conversion within current sheets in the earth's quasi-parallel magnetosheath. *Geophysical Research Letters*, *48*, e2020GL091859. <https://doi.org/10.1029/2020GL091859>

Received 25 NOV 2020
 Accepted 14 JAN 2021

Energy Conversion Within Current Sheets in the Earth's Quasi-Parallel Magnetosheath

Steven J. Schwartz^{1,2} , Harald Kucharek³ , Charles J. Farrugia³ , Karlheinz Trattner¹ , Imogen Gingell⁴ , Robert E. Ergun¹ , Robert Strangeway⁵ , and Daniel Gershman⁶ 

¹Laboratory for Atmospheric and Space Physics, Boulder, CO, USA, ²Also Emeritus Professor, Imperial College London, London, UK, ³University of New Hampshire, Durham, NH, USA, ⁴Physics and Astronomy, University of Southampton, Southampton, UK, ⁵UCLA, Los Angeles, CA, USA, ⁶Goddard Space Flight Center, Greenbelt, MD, USA

Abstract Shock waves in collisionless plasmas rely on kinetic processes to convert the primary incident bulk flow energy into thermal energy. That conversion is initiated within a thin transition layer but may continue well into the downstream region. At the Earth's bow shock, the region downstream of shock locations where the interplanetary magnetic field is nearly parallel to the shock normal is highly turbulent. We study the distribution of thin current events in this magnetosheath. Quantification of the energy dissipation rate made by the Magnetospheric Multiscale spacecraft shows that these isolated intense currents are distributed uniformly throughout the magnetosheath and convert a significant fraction (5%–11%) of the energy flux incident at the bow shock.

Plain Language Summary Shock waves form when a supersonic flow encounters an immovable object. Thus, ahead of the magnetic bubble formed by the Earth's extended magnetic field, the flow of charged particles emanating from the Sun known as the solar wind is shocked, slowed, and deflected around the Earth. In dense fluids, the conversion of the incident bulk flow energy into heat is accomplished by collisions between particles or molecules. However, the solar wind is so rarefied that such collisions are negligible, and the energy conversion involves more than one kinetic process that couples the different particles to the electromagnetic fields. Under some orientations of the interplanetary magnetic field carried by the wind, the shocked medium is highly turbulent. Within that turbulence are isolated thin regions carrying large electric currents. We have studied those currents, and found that they are converting energy from one form to another at a rate that is a significant fraction of the incident energy flux. Thus, these currents contribute significantly to the overall shock energetics.

1. Introduction

Shock waves in astrophysical plasma are almost always operating on scales that are much smaller than the particle collisional mean free path. Such collisionless shocks require plasma kinetic processes to decelerate the dominant incident bulk flow and “dissipate” that incident energy flux. These processes operate differently on the different plasma species and electromagnetic fields, and over different scales. They are responsible for preferential heating together with the acceleration to high energies of sub-populations of particles (Kucharek et al., 2003). The bow shock formed by the interaction of the supersonic solar wind flow with the Earth's magnetosphere has long been a prime laboratory for investigating collisionless shock physics thanks to its accessibility by ever-increasing high quality in situ satellite observations (Burgess & Scholer, 2015; Krasnoselskikh et al., 2013; Schwartz, 2006; Schwartz et al., 2013; Scudder et al., 1986; Stone & Tsurutani, 1985; Tsurutani & Stone, 1985).

The orientation of the upstream (unshocked) magnetic field plays a critical role in the physics of collisionless shocks. At quasi-parallel shocks, in which the angle θ_{Bn} between that field and the vector normal to the shock is less than 45° , the particle gyration around the magnetic field is unable to confine particles on the scale of their Larmor radii due to their mobility parallel to the field. The result is an extended “foreshock” region (Eastwood et al., 2005) where backstreaming particles drive instabilities that result in large-amplitude magnetic disturbances and attendant accelerated particles.

The region downstream of the quasi-parallel shock (Burgess et al., 2005) is also much more turbulent than that behind a quasi-perpendicular shock. This quasi-parallel magnetosheath is of interest for several reasons. First, recent work by Matthaeus et al. (2020) has considered it from the perspective of fundamental turbulence, comparing the turbulence spectrum and properties to the fully developed turbulence found in solar wind. The sheath turbulence is somewhat intermittent, implying that there are coherent structures embedded within it. They re-cast the energy equations, isolating terms in a “ $\Pi - D$ ” formulation to distinguish different channels of energy exchange, such as adiabatic compression, that may serve as pathways to dissipation. They do not find any strong correlation between the different terms in their formulation and, for example, regions of intense currents.

Retinò et al. (2007) reported early evidence of localized current sheets that were in the process of magnetically reconnecting. In the context of turbulence in collisionless plasmas, reconnection is thought to be a possible mechanism for the dissipation of energy that has cascaded from larger scales down to kinetic scales. Sundkvist et al. (2007) extended this work by a study of thin, possibly reconnecting current sheets selected by magnetic shear within the magnetosheath. There they focused specifically on the role of these current sheets in the dissipation of the turbulent energy cascade.

Magnetic reconnection also relaxes the field topology as it heats or accelerates the particles. More recently, using high-resolution data from the Magnetospheric Multiscale (MMS) mission, Phan et al. (2018) found examples in the magnetosheath of reconnecting current sheets at small, electron scales in which only the electrons participate in the reconnection process. This work highlights the electron-only microphysics within complex turbulent environments. By contrast, reconnection on larger scales associated with macroscopic boundaries and topological changes, such as that at the magnetopause, results in ion acceleration and jets at scales larger than the electron diffusion region. Ongoing work, (e.g, Wilder et al., 2018; Stawarz et al., 2019), has pursued the reconnection process, associated turbulence and statistics within the magnetosheath.

Gingell et al. (2019) found small-scale reconnection events within the transition layer at a quasi-parallel shock in both MMS data and simulation results. Wang et al. (2019) and Bessho et al. (2020) have extended these results to other shock geometries. These current sheets appear to be localized at/near the shock itself (Gingell et al., 2020) and are believed to represent a collisionless mechanism that contributes to the overall shock dissipation and field topology relaxation, driving the system toward a more homogeneous equilibrium plasma state.

To date, there has not been a comprehensive study of the specific role of thin current structures in energy re-distribution throughout the magnetosheath. This is clearly related to the turbulence laboratory that this region of geospace offers, as probed by Sundkvist et al. (2007). However, here we focus on the fact that the magnetosheath represents the downstream state of the bow shock, and a state that is still far from the uniform thermal equilibrium of textbook shocks in collisional fluids. We shall address the question: What role do small intense current structures downstream of the quasi-parallel shock play in the overall shock energetics? We address this question through a relatively unique volume of burst mode data taken during a single traversal of the sub-solar magnetosheath by the MMS spacecraft.

The next section summarizes both the data and our primary analysis methods. We then present our Results and provide some Discussion before drawing our final Conclusions.

2. Data and Methodology

Our primary results are drawn from the MMS mission (Burch et al., 2016). We also used data from both the Wind and Artemis spacecraft to establish the prevailing interplanetary conditions. An overview of the traversal of the terrestrial magnetosheath is shown in Figure 1, with the burst-mode data expanded in Figure 2. The analysis relies on data from the Fast Plasma Investigation (FPI; Pollock et al., 2016), Fluxgate Magnetometer (FGM; Russell et al., 2016) and electric field instrumentation (Ergun et al., 2016; Lindqvist et al., 2016; Torbert et al., 2016). We will concentrate on the latter half of this outbound traversal which corresponds to conditions behind the quasi-parallel shock under steady interplanetary conditions (see Figures 1g and S1 in the Supporting Information). The MMS trajectory was nearly radial and encountered the bow shock close to the sub-solar point (Figure 1h). Figure 1 shows that the quasi-parallel magnetosheath is

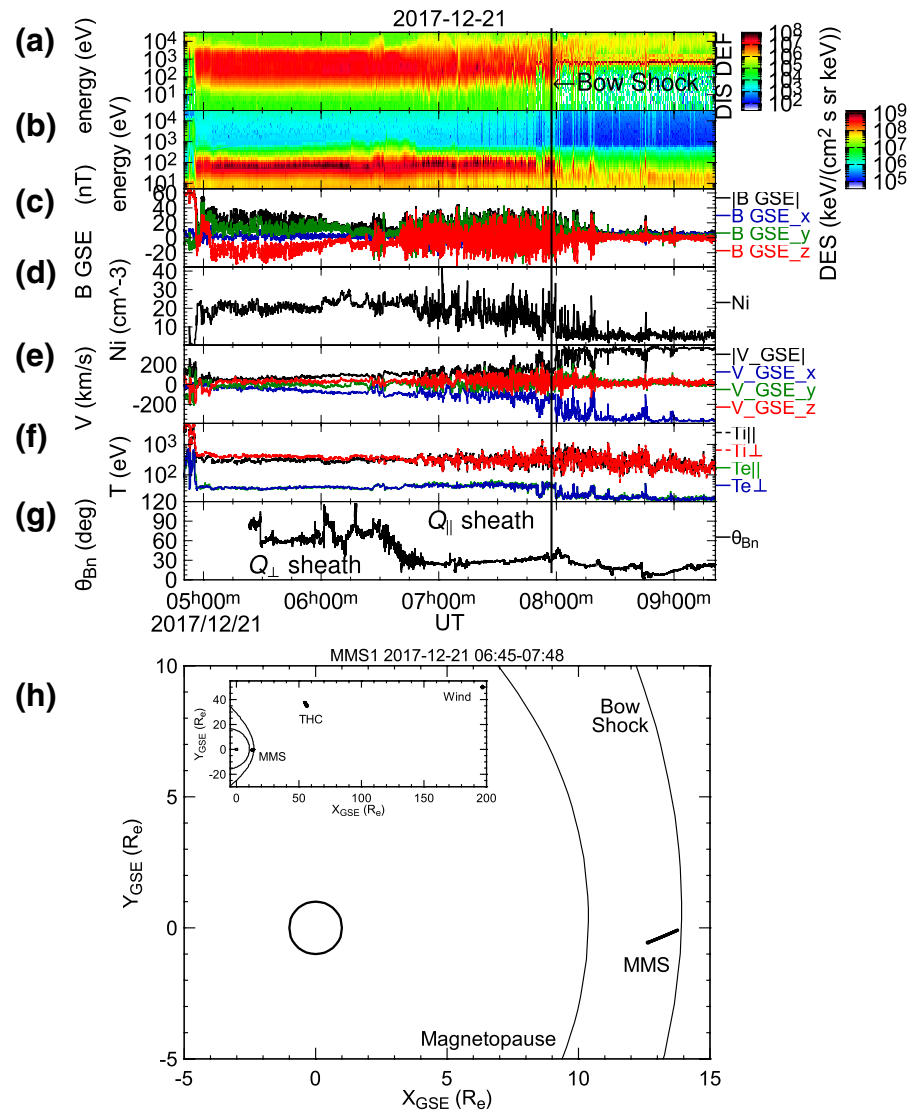


Figure 1. Top: Overview of the magnetosheath crossing by MMS1 on 2017/12/21. Ion (a) and electron (b) differential energy fluxes, (c) magnetic field in GSE, (d) ion density (e) ion flow velocity (f) electron and ion temperatures parallel and perpendicular to the local magnetic field and (g) angle between the interplanetary magnetic field (lagged in time from the WIND spacecraft) and the normal to a model of the Earth's bow shock. Bottom: (h) Trajectory of MMS showing an essentially sub-solar traversal of the magnetosheath together with (inset) the locations of THC (Artemis) and Wind spacecraft which were used to determine the lagged interplanetary plasma conditions. The four MMS spacecraft were separated by ~ 25 km. MMS, Magnetospheric Multiscale.

highly turbulent, and that there is ongoing deceleration, compression and heating with distance behind the bow shock. Fortunately, MMS burst mode data are available almost continuously (see Figure 2) throughout this encounter with the turbulent quasi-parallel sheath region.

The solar wind parameters deduced from Wind (averaged over a 25 min interval shown in Figure S1 of the Supporting Information) are number density $n = 3.34 \text{ cm}^{-3}$, proton and electron temperatures $T_p = 4.55 \text{ eV}$, $T_e = 13.9 \text{ eV}$, speed $V_{sw} = 400 \text{ km/s}$, and average GSE magnetic field vector $\mathbf{B} = (4.08, 1.51, 0.079) \text{ nT}$ with $|\mathbf{B}| = 4.35 \text{ nT}$. The normal to the bow shock, found by scaling a model bow shock (Slavin & Holzer, 1981; Schwartz, 1998) to the MMS crossing, was $(0.993, 0.036, 0.111)\text{GSE}$, reflecting the location very near to the sub-solar point. These values lead to a plasma $\beta = 1.3$ with electron $\beta_e = 0.3$ and ion $\beta_i = 1.0$, an Alfvén mach number of 7.7 and a fast magnetosonic mach number of 6.5. The shock geometry was $\theta_{Bn} \sim 19^\circ$.

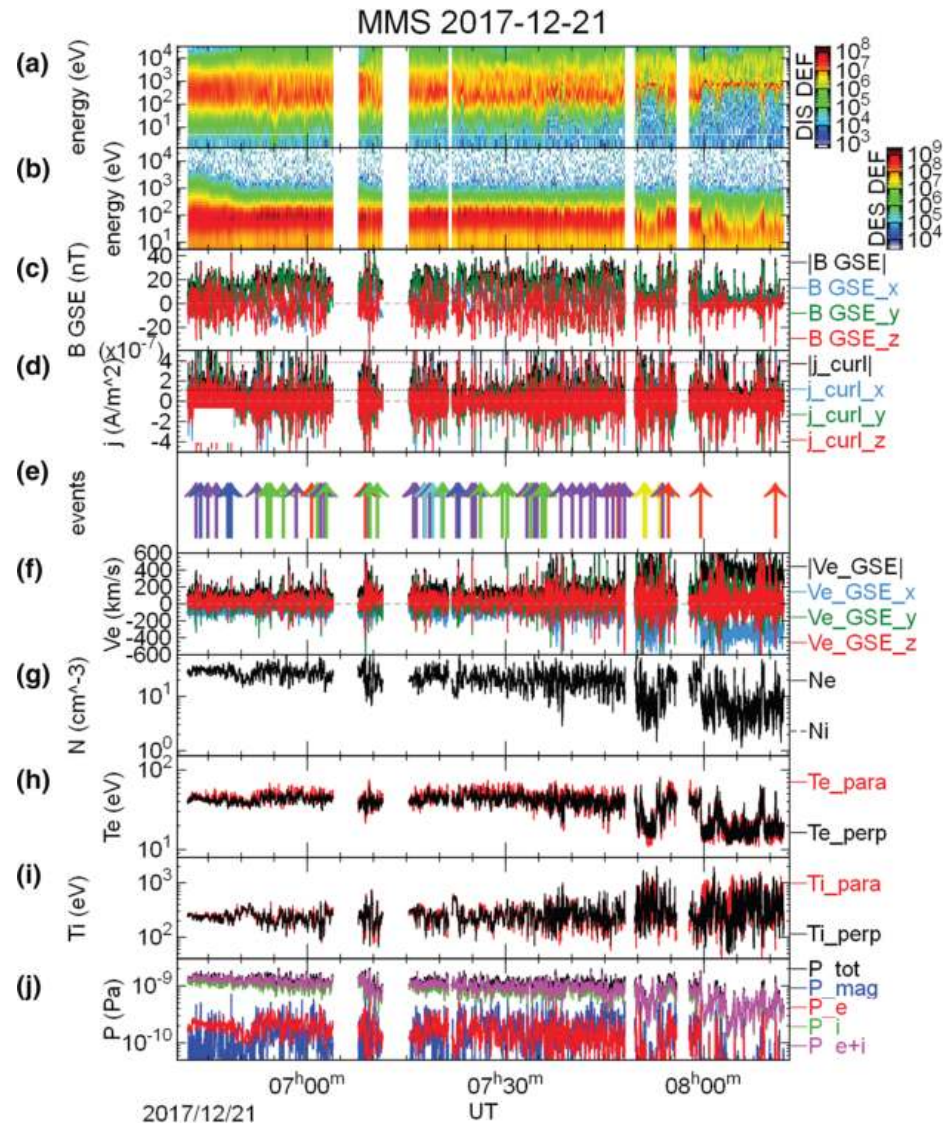


Figure 2. Overview of the burst-mode data from the MMS quasi-parallel sheath crossing observed on 2017-12-21. All data are from MMS1 except the current density. Ion (a) and electron (b) differential energy fluxes in $\text{keV}/(\text{cm}^2 \text{sr keV})$ (c) magnetic field in GSE, (d) electric current density calculated from a curlometer technique. Dotted lines show the 1σ and 3σ $|j|$ levels (e) selected events with $|j| > 3\sigma$, color coded by probable type of current structure (see text and Figure 4 below) (f) electron bulk flow velocity (g) electron and ion plasma densities (indistinguishable on this scale) (h) electron and (i) ion temperatures parallel and perpendicular to the local magnetic field and (j) plasma, field and total pressure. MMS, Magnetospheric Multiscale.

We use the curlometer four-spacecraft method (Chanteur, 1998; Dunlop & Eastwood, 2008) to determine the electric current density \mathbf{j} . We take advantage of the 30 ms FPI electron measurements to compute the electric field $\mathbf{E}' = \mathbf{E} + \mathbf{v}_e \times \mathbf{B}$ in the electron rest frame smoothed to match the 30 ms electron cadence, where \mathbf{v}_e is the bulk electron fluid velocity and \mathbf{B} is the magnetic field. We calculate \mathbf{E}' at the barycenter of the tetrahedron by combining data from the four spacecraft, to match the curlometer estimation of \mathbf{j} . We then calculate the energy conversion (Swisdak et al., 2018) between fields and particles, namely $\mathbf{j} \cdot \mathbf{E}'$. Positive values of $\mathbf{j} \cdot \mathbf{E}'$ correspond to energy conversion from the fields to the particles. Note that, apart from the lower cadence of the data, employing the ion velocity instead of \mathbf{v}_e will lead to the same energy transfer rate, as the difference between the two expressions is $\mathbf{j} \cdot (\mathbf{v}_i - \mathbf{v}_e) \times \mathbf{B} \propto \mathbf{j} \cdot \mathbf{j} \times \mathbf{B} = 0$ in a singly ionized plasma (Zenitani et al., 2011). Other MMS data shown are drawn from MMS1.

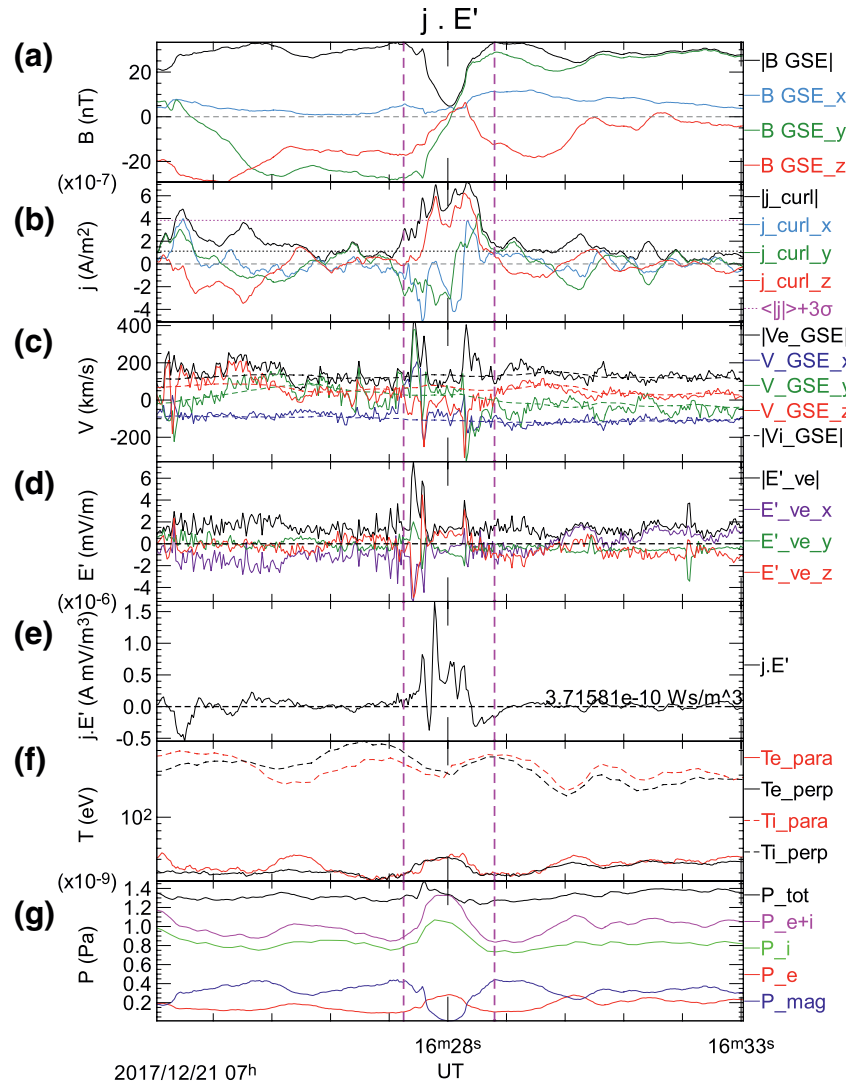


Figure 3. An example of the current sheets/structures selected for this study. Data from MMS1 except in (b) and (e) Top to bottom (a) magnetic field in GSE (b) current density \mathbf{j} in GSE calculated via the curlmeter method (c) electron (solid) and ion (dashed) bulk flow velocities (d) DC electric field transformed into the electron flow frame (e) energy conversion rate $\mathbf{j} \cdot \mathbf{E}'$ based on \mathbf{E}' calculated at the barycenter of the four spacecraft tetrahedron (f) electron (solid) and ion (dashed) temperatures parallel (red) and perpendicular (black) to the instantaneous magnetic field (g) magnetic, particle, and total plasma pressure. Note the current density rises above the dashed 3σ line in panel (b), and the region surrounding this selected manually as the full event delineated by dashed vertical magenta lines. The integral of $\mathbf{j} \cdot \mathbf{E}'$ over the event is shown in panel (e). MMS, Magnetospheric Multiscale.

Our event selection identifies instances of high current densities, specifically ones in which the magnitudes are 3σ above the average for the entire interval. We then select manually the region surrounding that peak in \mathbf{j} that captures the full current structure. One such example is shown in Figure 3. The Supporting Information includes similar plots for all 59 events. This event displays a near magnetic null coincident with a reversal in the B_y component, reminiscent of reconnecting current sheets (Burch et al., 2016). There is a rise in the particle pressures (panel g) due primarily to a rise in density (not shown), as the ion temperature decreases there. Total pressure balance is maintained across the event. There is a clear signature in $\mathbf{j} \cdot \mathbf{E}'$ (panel e) which is much reduced outside the event even where there are significant current and field values. We are primarily interested in the contribution of these events to the energy budget mediated by the bow shock and its evolution within the magnetosheath. Toward that end, we have integrated $\mathbf{j} \cdot \mathbf{E}'$ across the event, shown in the text label in Figure 3e.

As can be seen in Figure 2e, the 3σ events are distributed roughly uniformly throughout the turbulent sheath interval, so either an individual event survives this entire traversal or, more likely, it lasts some time and is replaced by an equivalent structure. Since the spacecraft is moving slowly with respect to the sheath flow, a time average is equivalent to a spatial average within the turbulent sheath. Thus the average energy conversion rate per unit volume in the magnetosheath is simply the sum of $\mathbf{j} \cdot \mathbf{E}'$ integrated across all the observed events divided by the total observation time T_{obs} , that is,

$$\varepsilon = \frac{1}{T_{obs}} \sum \int \mathbf{j} \cdot \mathbf{E}' dt \quad (1)$$

We assume for simplicity that the events are all locally planar current sheets and oriented perpendicular to a constant sheath flow. We have explored the event orientation for the subset that appear to be tangential structures, namely those which appear to be either reconnecting current sheets or passive tangential discontinuities. The results are presented in the Discussion section below, and suggest an uncertainty of 30% in our estimates of the energy conversion rate.

Using our assumption of planar, perpendicularly oriented current sheets, the volume of the sheath is proportional to the distance L throughout which the exchange (1) is occurring, so the energy conversion rate per unit area, compared to the incident ram energy flux at the bow shock, is:

$$\frac{F_L}{F_{SW}} = \frac{(L / T_{obs}) \sum \int \mathbf{j} \cdot \mathbf{E}' dt}{V_{sw} \rho V_{sw}^2 / 2} \quad (2)$$

3. Results

We looked at 59 current structures that matched our 3σ of $\langle |\mathbf{j}| \rangle$ selection criterion. These included 27 events with magnetic depressions/near nulls, as that in Figure 3 and possible electron velocity jets parallel to the reversing field as found in magnetic reconnection sites, 14 which appeared to be tangential discontinuities lacking a dip in $|\mathbf{B}|$ and with constant total pressure, 3 which resembled rotational discontinuities with constant magnetic field strength, 6 which were reminiscent of flux ropes with a peak in $|\mathbf{B}|$ and total pressure, 3 which resembled steepened ULF waves with trailing wavetrains and 6 others. This classification is based on a qualitative assessment of variations of the parameters by inspection of plots identical in format to Figure 3, and is shown in Table S1 of the Supporting Information for all events together with the individual energy conversion values. We have not attempted a detailed analysis of, for example, the traditional lmn geometry for each event; we provide the event details in the Supporting Information for use in future studies. The number of possibly reconnecting current sheets over this 90 min period is similar to that found by Sundkvist et al. (2007) over a similar length of data from the Cluster data.

The 59 events have an average duration of 2.8 s. Taken together, they make up only 3% of the roughly 90 min quasi-parallel magnetosheath traversal in which they were observed. Based on our assumption that the events are planar, they thus fill $\sim 3\%$ of the volume of the magnetosheath. Can such a small volume process a significant amount of energy?

Figure 4 summarizes the energy conversion statistics for all the events. Most of the events (nearly 75%) have positive integrated $\mathbf{j} \cdot \mathbf{E}'$ indicating that they convert field energy into particle energy on the average. Summing over all 59 events, Equation 2 reveals that the net conversion of 4.0×10^{-9} Ws/m³ corresponds to $\sim 5\%$ of the incident solar wind ram energy flux. By way of comparison, the rise in electron enthalpy flux ($\equiv V_{flow} [\gamma / (\gamma - 1)] nk_B T_e$) with $\gamma = 5/3$ across the bow shock itself is $\sim 20\%$ of the ram energy flux, while the increase in electron enthalpy flux from just downstream of the bow shock (at 07:50 where $T_e \sim 40$ eV) to the downstream edge of the quasi-parallel magnetosheath (at 06:45 where $T_e \sim 55$ eV) represents $\sim 7.5\%$ of that same incident ram energy flux. These comparisons reveal that the isolated current events studied here are energetically comparable to both the heating at the bow shock itself and to the continued increase in electron temperature with downstream distance. We discuss below the caution that should be applied here since $\mathbf{j} \cdot \mathbf{E}'$ is the total energy conversion, including bulk flow, adiabatic compression and irreversible dissipation.

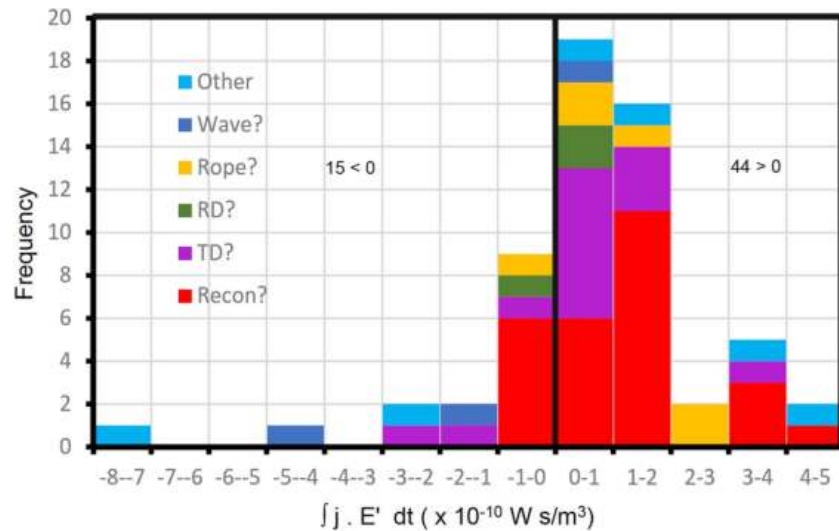


Figure 4. Statistics of the integrated energy conversion $\int \mathbf{j} \cdot \mathbf{E}' dt$ for the 59 events in this study, broken down by the apparent type of the event (see text).

As a final note here, we have seen that these current events can have both positive and negative energy conversions. In terms of their overall impact on the energetics of the sheath, we have calculated the total energy processed by the events regardless of sign by summing $|\mathbf{j} \cdot \mathbf{E}'|$. This conversion is $8.9 \times 10^{-9} \text{ W s/m}^3$, corresponding to 11% of the incident ram energy flux.

4. Discussion

Our results show that isolated current structures within the magnetosheath downstream of the quasi-parallel bow shock convert electromagnetic field energy into particle energy at a rate that is comparable to the increase in electron enthalpy flux within the magnetosheath, and 25% of the change in that enthalpy flux occurring at the shock itself. If that conversion is all irreversible, this implies that roughly 20% of the electron heating from the solar wind to deep in the magnetosheath is (a) distributed throughout the magnetosheath and (b) localized in space to the most intense currents. However, the electro-fluid dynamics can't distinguish irreversible heating from reversible compression or accelerated flows. Recent work in the context of plasma turbulence (Matthaeus et al., 2020) has attempted to separate out these different energy reservoirs. They conclude that there is no direct correlation between the intense current sheets and their $\Pi - D$ measure of energy conversion (Bandyopadhyay et al., 2020), although they do find that conversion is highly spatially localized near to intense current events. We note in this context that most of our events, such as that shown in Figure 3, do not show significant temperature changes within them.

However, our goal here is simpler, namely to establish whether intense currents are significant in terms of the overall shock and sheath energetics. For the case studied here the total energy conversion (ignoring the sign) is approximately 11% of the ram energy flux incident at the bow shock. This is indicative of the incompleteness of the bow shock in thermalizing the incident ram energy and of the ongoing dissipation, redistribution, and relaxation of the plasma through the entire magnetosheath. Yet this specific energy conversion is mediated by only $\sim 3\%$ of the volume of the magnetosheath. Interestingly, a particle-in-cell study of turbulence (Wan et al., 2016) finds similar numbers, for example, that 3σ current intensities occupy $\sim 2\%$ of their simulation domain and account for $\sim 35\%$ of the total dissipation (Wan et al., 2016, Figure 3c).

Our analysis (cf. Equation 2) assumed that the intense current events were planar sheets oriented perpendicular to the plasma flow. For all our events which appear to have a tangential structure, namely those which we classed as possibly reconnecting or as non-reconnecting tangential discontinuities, we have estimated the actual orientation of the underlying current sheet by the cross product between the pre and post event fields, averaged over the 1-s intervals immediately adjacent to the event. This is only an estimate, as for many of the events the fields are not steady during these intervals. Within this sub-group (41 events)

the average angle between this estimated orientation and the mean ion velocity vector within the event is 50°. We have estimated the individual event energy conversion reduced by the cosine of the corresponding orientation angle of the current sheet. Summed over this subset of events, the net energy conversion rate is reduced by 30% relative to the equivalent sum for an assumed perpendicular orientation. Table S1 in the Supporting Information includes the individual event orientation angles together with the pre- to post-event magnetic shear angle for this subset. These results are roughly consistent with a random orientation of the individual current sheets, and do not reveal any systematic bias that would disrupt our overall qualitative and quantitative conclusions.

5. Conclusions

We have studied the exchange between particle and electromagnetic energy downstream of the quasi-parallel Earth's bow shock through the analysis of a traversal of the sub-solar magnetosheath by MMS. The interplanetary conditions were steady, and an unusually long interval of burst mode data was available. Our main conclusion is that thin current events or sheets, which are approximately 3 s in duration and thus occupy 3% of the magnetosheath volume, process nearly 11% of the bulk flow ram energy incident at the bow shock. In this example, that energy conversion was predominantly from field energy to particle energy. We are not able to determine whether that represents irreversible dissipation or reversible compressions (Matthaeus et al., 2020), nor the partition of that particle energy between electrons and ions. Nonetheless, our results show the importance of these isolated thin current structures in the energy processing that is initiated at the bow shock but continues far into the downstream region.

The region downstream of a quasi-parallel shock is well-known to be turbulent (Burgess et al., 2005; Lucek et al., 2005) which promotes the formation of thin current structures. The fluctuation levels, and hence current sheet intensities, downstream of the quasi-perpendicular bow shock are much less. This can even be seen in the first third of Figures 1a–1f before the interplanetary field turned to more quasi-parallel geometries. These regions show less evolution in density compression or temperature, suggesting that the binding of the particles and fields by the perpendicular geometry promotes more rapid energy exchange. There may nonetheless be subtle changes within individual particle populations as, e.g., anisotropy-driven instabilities relax these populations toward thermal equilibrium. This could be productively explored in a similar future study of this kind. Upstream disturbances such as hot flow anomalies and foreshock bubbles, together with higher levels of interplanetary turbulence, may also lead to higher levels of magnetosheath turbulence which again could promote more numerous and intense current sheets even under quasi-perpendicular geometries.

Data Availability Statement

Artemis and Wind data were drawn from the SPDF/CDAWEB repository (<https://cdaweb.gsfc.nasa.gov/index.html/>). The authors gratefully acknowledge the respective instrument teams and archive curators. We profited from discussions with Alex Chasapis. MMS data can be found at the MMS public Science Data Center (<https://lasp.colorado.edu/mms/sdc/public/>). All the data analysis and graphics were performed using the opensource QSAS Science Analysis System (<https://sourceforge.net/projects/qsas/>).

Acknowledgments

This work was supported by NASA Award 80NSSC19K0849 together with NASA MMS contracts to the instrument teams. IG is supported by a Royal Society URF.

References

- Bandyopadhyay, R., Matthaeus, W. H., Parashar, T. N., Yang, Y., Chasapis, A., Giles, B. L., et al. (2020). Statistics of kinetic dissipation in the earth's magnetosheath: MMS observations. *Physical Review Letters*, *124*(25), 255101. <https://doi.org/10.1103/PhysRevLett.124.255101>
- Bessho, N., Chen, L. J., Wang, S., Hesse, M., Wilson, I., Wilson, L. B., & Ng, J. (2020). Magnetic reconnection and kinetic waves generated in the Earth's quasi-parallel bow shock. *Physics of Plasmas*, *27*(9), 092901. <https://doi.org/10.1063/5.0012443>
- Burch, J. L., Moore, T. E., Torbert, R. B., & Giles, B. L. (2016). Magnetospheric multiscale overview and science objectives. *Space Science Reviews*, *199*(1–4), 5–21. <https://doi.org/10.1007/s11214-015-0164-9>
- Burch, J. L., Torbert, R. B., Phan, T. D., Chen, L. J., Moore, T. E., Ergun, R. E., et al. (2016). Electron-scale measurements of magnetic reconnection in space. *Science*, *352*(6290), aaf2939-1–aaf2939-10. <https://doi.org/10.1126/science.aaf2939>
- Burgess, D., Lucek, E. A., Scholer, M., Bale, S. D., Balikhin, M. A., Balogh, A., et al. (2005). Quasi-parallel shock structure and processes. *Space Science Reviews*, *118*(1–4), 205–222. <https://doi.org/10.1007/s11214-005-3832-3>
- Burgess, D., & Scholer, M. (2015). *Collisionless shocks in space plasmas*, Cambridge, UK: Cambridge University Press. <https://doi.org/10.1017/CBO9781139044097>

- Chanteur, G. (1998). Spatial interpolation for four spacecraft: Theory. *Analysis Methods for Multi-Spacecraft Data*, ISSI Scientific Reports Series (1.1 ed., Vol. 1., pp. 349–370). Noordwijk, The Netherlands: ESA Publications Division for International Space Science Institute. Retrieved from http://www.issibern.ch/PDF-Files/analysis_methods_1_1a.pdf
- Dunlop, M. W., & Eastwood, J. P. (2008). The curlometer and other gradient based methods. *Ionospheric Multi-Spacecraft Analysis Tools*, ISSI Scientific Reports Series (Vol. 8, pp. 17–26). Switzerland: Springer, Cham. https://doi.org/10.1007/978-3-030-26732-2_5
- Eastwood, J. P., Lucek, E. A., Mazelle, C., Meziane, K., Narita, Y., Pickett, J., & Treumann, R. A. (2005). The Foreshock. *Space Science Reviews*, 118(1–4), 41–94. <https://doi.org/10.1007/s11214-005-3824-3>
- Ergun, R. E., Tucker, S., Westfall, J., Goodrich, K. A., Malaspina, D. M., Summers, D., et al. (2016). The axial double probe and fields signal processing for the MMS mission. *Space Science Reviews*, 199(1–4), 167–188. <https://doi.org/10.1007/s11214-014-0115-x>
- Gingell, I., Schwartz, S. J., Eastwood, J. P., Burch, J. L., Ergun, R. E., Fuselier, S., et al. (2019). Observations of magnetic reconnection in the transition region of quasi-parallel shocks. *Geophysical Research Letters*, 46(3), 1177–1184. <https://doi.org/10.1029/2018GL081804>
- Gingell, I., Schwartz, S. J., Eastwood, J. P., Stawarz, J. E., Burch, J. L., Ergun, R. E., et al. (2020). Statistics of reconnecting current sheets in the transition region of earth's bow shock. *Journal of Geophysical Research*, 125(1), e27119. <https://doi.org/10.1029/2019JA027119>
- Krasnoselskikh, V., Balikhin, M., Walker, S. N., Schwartz, S. J., Sundkvist, D., Lobzin, V., et al. (2013). The dynamic quasiperpendicular shock: Cluster discoveries. *Space Science Reviews*, 178(2–4), 535–598. <https://doi.org/10.1007/s11214-013-9972-y>
- Kucharek, H., Möbius, E., Li, W., Farrugia, C. J., Popecki, M. A., Galvin, A. B., et al. (2003). On the source and acceleration of energetic He⁺: A long-term observation with ACE/SEPICA. *Journal of Geophysical Research*, 108(A10), 8040. <https://doi.org/10.1029/2003JA009938>
- Lindqvist, P.-A., Olsson, G., Torbert, R. B., King, B., Granoff, M., Rau, D., et al. (2016). The spin-plane double probe electric field instrument for MMS. *Space Science Reviews*, 199(1–4), 137–165. <https://doi.org/10.1007/s11214-014-0116-9>
- Lucek, E. A., Constantinescu, D., Goldstein, M. L., Pickett, J., Pinçon, J. L., Sahraoui, F., et al. (2005). The Magnetosheath. *Space Science Reviews*, 118(1–4), 95–152. <https://doi.org/10.1007/s11214-005-3825-2>
- Matthaeus, W. H., Yang, Y., Wan, M., Parashar, T. N., Bandyopadhyay, R., Chasapis, A., et al. (2020). Pathways to dissipation in weakly collisional plasmas. *The Astrophysical Journal*, 891(1), 101. <https://doi.org/10.3847/1538-4357/ab6d6a>
- Phan, T. D., Eastwood, J. P., Shay, M. A., Drake, J. F., Sonnerup, B. U. Ö., Fujimoto, M., et al. (2018). Electron magnetic reconnection without ion coupling in Earth's turbulent magnetosheath. *Nature*, 557(7704), 202–206. <https://doi.org/10.1038/s41586-018-0091-5>
- Pollock, C., Moore, T., Jacques, A., Burch, J., Gliese, U., Saito, Y., et al. (2016). Fast plasma investigation for magnetospheric multiscale. *Space Science Reviews*, 199(1–4), 331–406. <https://doi.org/10.1007/s11214-016-0245-4>
- Retinò, A., Sundkvist, D., Vaivads, A., Mozer, F., André, M., & Owen, C. J. (2007). In situ evidence of magnetic reconnection in turbulent plasma. *Nature Physics*, 3(4), 236–238. <https://doi.org/10.1038/nphys574>
- Russell, C. T., Anderson, B. J., Baumjohann, W., Bromund, K. R., Dearborn, D., Fischer, D., et al. (2016). The magnetospheric multiscale magnetometers. *Space Science Reviews*, 199, 189–256. <https://doi.org/10.1007/s11214-014-0057-3>
- Schwartz, S. J. (1998). Shock and discontinuity normals, mach numbers, and related parameters. *Analysis Methods for Multi-Spacecraft Data Analysis*, ISSI Scientific Reports Series, (1.1 ed., Vol. 1., pp. 249–270). Noordwijk, The Netherlands: ESA Publications Division for International Space Science Institute. Retrieved from http://www.issibern.ch/PDF-Files/analysis_methods_1_1a.pdf
- Schwartz, S. J. (2006). Shocks: Commonalities in solar-terrestrial chains. *Space Science Reviews*, 124(1–4), 333–344. <https://doi.org/10.1007/s11214-006-9093-y>
- Schwartz, S. J., Zweibel, E. G., & Goldman, M. (2013). Microphysics in astrophysical plasmas. *Space Science Reviews*, 178(2–4), 81–99. <https://doi.org/10.1007/s11214-013-9975-8>
- Scudder, J. D., Mangeney, A., Lacombe, C., Harvey, C. C., Wu, C. S., & Anderson, R. R. (1986). The resolved layer of a collisionless, high β , supercritical, quasi-perpendicular shock wave, 3. Vlasov electrodynamics. *Journal of Geophysical Research*, 91(A10), 11075–11098. <https://doi.org/10.1029/JA091iA10p11075>
- Slavin, J. A., & Holzer, R. E. (1981). Solar wind flow about the terrestrial planets, 1. Modeling bow shock position and shape. *Journal of Geophysical Research*, 86(A13), 11401–11418. <https://doi.org/10.1029/JA086iA13p11401>
- Stawarz, J. E., Eastwood, J. P., Phan, T. D., Gingell, I. L., Shay, M. A., Burch, J. L., et al. (2019). Properties of the turbulence associated with electron-only magnetic reconnection in Earth's magnetosheath. *The Astrophysical Journal Letters*, 877(2), L37. <https://doi.org/10.3847/2041-8213/ab21c8>
- Stone, R. G., & Tsurutani, B. T. (1985). *Collisionless shocks in the heliosphere: A tutorial review*. Washington DC American Geophysical Union Geophysical Monograph Series, 34. <https://doi.org/10.1029/GM034>
- Sundkvist, D., Retinò, A., Vaivads, A., & Bale, S. D. (2007). Dissipation in turbulent plasma due to reconnection in thin current sheets. *Physical Review Letters*, 99(2), 025004. <https://doi.org/10.1103/PhysRevLett.99.025004>
- Swisdak, M., Drake, J. F., Price, L., Burch, J. L., Cassak, P. A., & Phan, T. D. (2018). Localized and intense energy conversion in the diffusion region of asymmetric magnetic reconnection. *Geophysical Research Letters*, 45(11), 5260–5267. <https://doi.org/10.1029/2017GL076862>
- Torbert, R. B., Russell, C. T., Magnes, W., Ergun, R. E., Lindqvist, P.-A., LeContel, O., et al. (2016). The FIELDS instrument suite on mms: scientific objectives, measurements, and data products. *Space Science Reviews*, 199(1–4), 105–135. <https://doi.org/10.1007/s11214-014-0109-8>
- Tsurutani, B. T., & Stone, R. G. (1985). *Collisionless shocks in the heliosphere: Reviews of current research*. Washington DC American Geophysical Union Geophysical Monograph Series, 35. <https://doi.org/10.1029/GM035>
- Wang, S., Chen, L.-J., Bessho, N., Hesse, M., Wilson, L. B., Giles, B., et al. (2019). Observational evidence of magnetic reconnection in the terrestrial bow shock transition region. *Geophysical Research Letters*, 46(2), 562–570. <https://doi.org/10.1029/2018GL080944>
- Wan, M., Matthaeus, W. H., Roytershteyn, V., Parashar, T. N., Wu, P., & Karimabadi, H. (2016). Intermittency, coherent structures and dissipation in plasma turbulence. *Physics of Plasmas*, 23(4), 042307. <https://doi.org/10.1063/1.4945631>
- Wilder, F. D., Ergun, R. E., Burch, J. L., Ahmadi, N., Eriksson, S., Phan, T. D., et al. (2018). The role of the parallel electric field in electron-scale dissipation at reconnecting currents in the magnetosheath. *Journal of Geophysical Research*, 123(8), 6533–6547. <https://doi.org/10.1029/2018JA025529>
- Zenitani, S., Hesse, M., Klimas, A., & Kuznetsova, M. (2011). New measure of the dissipation region in collisionless magnetic reconnection. *Physical Review Letters*, 106(19), 195003. <https://doi.org/10.1103/PhysRevLett.106.195003>